Md. Abdus Sattar *et al*, International Journal of Advances in Agricultural Science & Technology,
Vol.10 Issue.2, Feb 2023, pg. 26-40

ISSN: 2348-1358
Impact Factor: 6.901
NAAS Rating: 3.77

EFFECTS OF MORPHOLOGY ON CHARGE TRANSFER PROPERTIES OF ULTRATHIN METALLIC FILMS ON GRAPHITE NANOSTRUCTURES

Md. Abdus Sattar

Abstract

Reportedly, the size and density of the metal nanoparticles considerably alter the work function on graphitic nanostructures coated with gold, platinum, and chromium. Nanoparticles of gold and platinum had surface potentials of 1.4 V and 0.6 V, respectively, much greater than the bulk metals' 0.45 V and 0.6 V, respectively. Surface potential (SP) measurements on chromium showed a sign inversion, with tiny nanoparticles measuring -2 V and bulk chromium -0.9 V. Consistent with the known doping qualities, the sign shift is shown to be caused by an inversion of the graphite Fermi level. Charge transfer from metal nanoparticles to graphitic nanostructure is confirmed by a link of surface potentials with the resultant dipole. For nanoparticles with a size between 0.1 nm and 1 nm, the charge transfer rose from 0.04 eV to 0.27 eV. These results show that the morphology of the film, in addition to the metal choice, may affect the electrical structure at the metal-graphene/graphite interface.

Key words: Nanoparticles, TEM, SAED, SKPM, Surface potential, Charge transfer.

1.0 Introduction

Clusek et al. (2009), Blanter and Martin (2007), Uchoa et al. (2008), Sutter et al. (2008), and Benayad et al. (2009) all point to the importance of charge transfer as an interfacial phenomena for graphene/graphite electronics and support catalysis. Clusek et al. (2009) and Giovannetti et al. (2008) found that this happens when the local density of state changes as a result of electron interaction between the metal and graphene surface. Multiple studies have shown that the work function of the contacting metal determines the magnitude of the Fermi level shift (Uchoa et al., 2008; Benayad et al., 2009; Liu et al., 2011). Photostron spectroscopy (Benayad et al., 2009; Pirkle et al., 2009; Obraztsov et al., 2002; Ohgi and Fujita, 2003; Hamada and Otani, 2010) and scanning tunnelling microscopy (STM) (Klusek et al., 2009; Li et al., 2009; Brar et al., 2007; Marchini et al., 2007) have shown these investigations. Additional interactions derived from the kind of bonding have been suggested in recent theoretical investigations using density function theory (DFT) (Uchoa et al., 2008; Giovannetti et al., 2008; Hamada and Otani, 2010; Gong et al., 2010; Huard et al., 2008). Charge transfer occurs when surface electrons delocalize for physio-adsorbed substances, and orbital hybridization occurs in graphite as a consequence of intense chemisorption (Giovannetti et al., 2008; Liu et al., 2011; Gong et al., 2010). According to Giovannetti et al. (2012), a dipole potential is generated when the surface's electrical structure changes.

ISSN: 2348-1358
Impact Factor: 6.901
NAAS Rating: 3.77

(Gomer, 1975; Gong et al., 2010; Liu et al., 2011). Hence, the direction of electron transfer crossover takes into account a factor of the contact distances and does not happen when the work function difference between graphite and metal is zero (Giovannetti et al., 2008; Gong et al., 2010; Jin et al., 2010). Standard principles of semiconductor physics provide no explanation for the unusual metal-doping behavior of graphite (Rusu et al., 2010; Somorjai, 1981). Up to this point, models have provided detailed descriptions of this interaction in the context of metal atoms packing as closely as possible on a graphite surface and achieving uniform monolayer coverage. Sun et al. (2010) and Gefen et al. (1986) found that the electrical characteristics of bulk metals and thin metal films are different. As an example, Ohgi and Fujita (2003) demonstrated that the number of conducting electrons may be changed by modifying the film shape, and that this amount determines the charge generated by Au connected with molecular layers. Different concentrations of metal atoms on graphite's surface might lead to different electronic states and chemical reactivities, which current models would not be able to account for.

2.0 Experimental procedure

A process of repetitive peeling was used to exfoliate graphite films made from synthetic highly ordered pyrolytic graphite (HOPG). The graphitic nanostructures were then covered with gold by means of thermal deposition at two distinct pressures (10-11 and 10-6 mbar). The sputtering process was also used to produce ultrathin films of Pt and Cr on other substrates. To acquire surface potentials, the scanning Kelvin probe microscopy (SKPM) method was used in both air and vacuum contexts. The parameters employed were a bandwidth of 300 KHz and a capacitance of 40 NM-1, and the tips were coated with either Au or Pt. In order to analyze the data, two separate approaches were developed for value extraction: (i) line profiles covering the whole scan range, with the average SP profile from each picture scan serving as the final value; and (ii) converting raw images to binary format and masking high contrast areas. That way, we could block out the huge fluctuations caused by individual points and be confident that all of our observations were consistent. The system was remeasured after being evacuated with air to rule out environmental influences. We used a transmission electron microscope (TEM) to look at the materials' morphology.

3.0 Results

3.1 Topography and Surface Potential Measurements

The results of two samples coated with 1 nm Au under identical circumstances are shown in Figure 1 as SKPM scans acquired with a Pt tip in vacuum. Obtaining histogram distributions throughout the whole scan allowed us to derive a representative value. Compared to both bulk Au and fresh graphite surface, the measured potentials are bigger, as shown by the arrows. We scanned the same spot twice and then did the same thing to two other parts of the same sample. The average of the mean distributions was used to derive the final result. Another sample was subjected to the same procedure under identical circumstances to guarantee repeatability. Surface potential scans showed a tightly packed histogram, with nanoparticles exhibiting a greater mean value than both fresh graphite and bulk gold.

ISSN: 2348-1358
Impact Factor: 6.901
NAAS Rating: 3.77

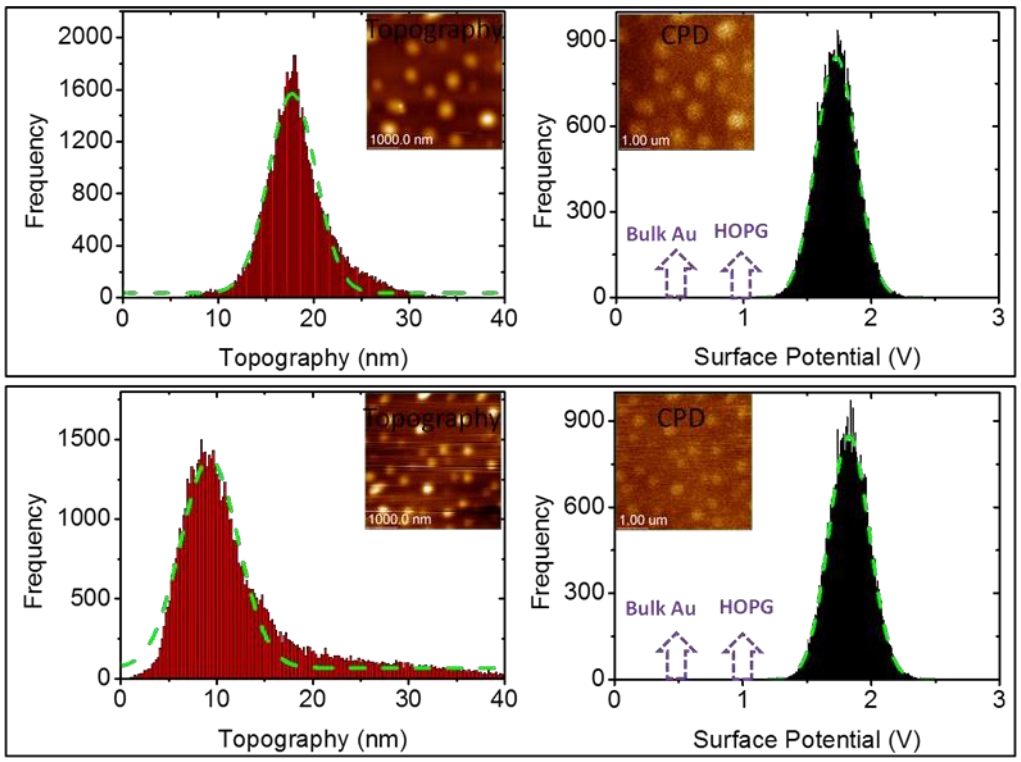

Fig. 1: Histogram distribution on topography and SP on two samples at similar conditions

3.2 Effect of Au nominal thickness

Graphitic films coated with gold exhibit SP values (Figure 2). Data consisting of 8, 16, and 8 values, respectively, are retrieved from histogram distributions, line profiles of raw pictures, and line profiles after masking high contrast regions. Masking high-contrast areas due to a consistent backdrop reduces the variation shown by the error bars. There are three parts to the SP curves: (i) the first is an exponential decline with increasing Au deposition, (ii) the value on thick film, and (iii) an initial rise up to 1.4 V for 1 nm deposition. Both the surface and bulk graphite films show a greater initial rise than SP when they are new.

ISSN: 2348-1358
Impact Factor: 6.901
NAAS Rating: 3.77

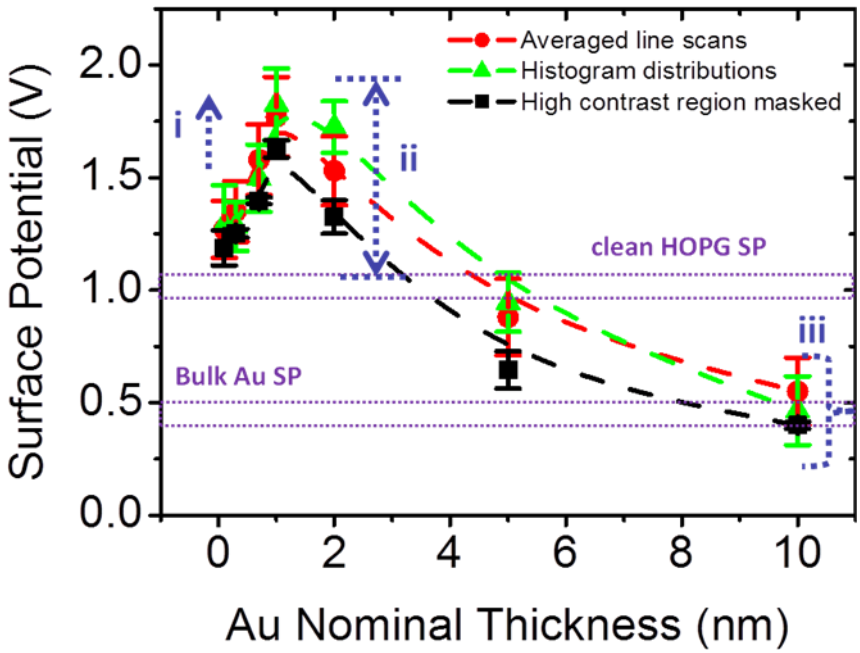

Fig. 2: Surface potential as a function of Au nominal thickness extracted from line averages, histogram distributions and masked high contrast regions.

In Fig. 3, we can see that the general trends are in accord when compared to Au films deposited at 10-6 mbar pressure for the same nominal thickness. When measuring thick films, the values are reliant on the metal tip, but when working with thin films, this is not the case. With a Pt tip, we measure values of 0.45 V, while with an Au tip, we measure values of 0.03 V.

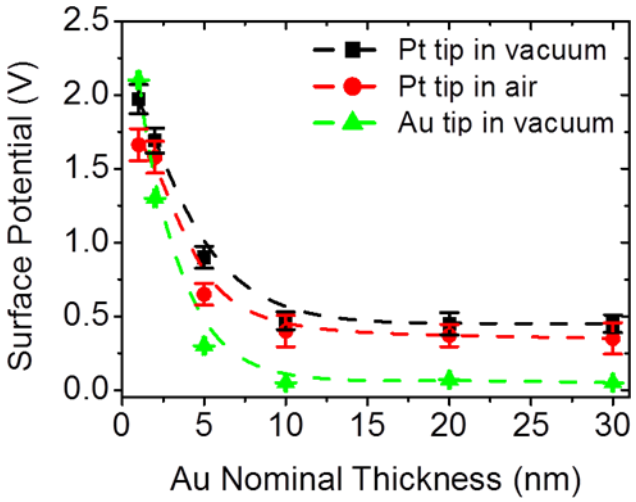

ISSN: 2348-1358
Impact Factor: 6.901
NAAS Rating: 3.77

Fig. 3: Surface potentials on Au deposited at 10-6 mbar pressure

Surface potentials on an Au film with a notional thickness of 1 nm are shown in Figure 4, after air venting of the system. Although the results were somewhat lower and showed substantial variability (depicted by error bars), the main trends were same when compared to observations in a vacuum (Fig. 2).

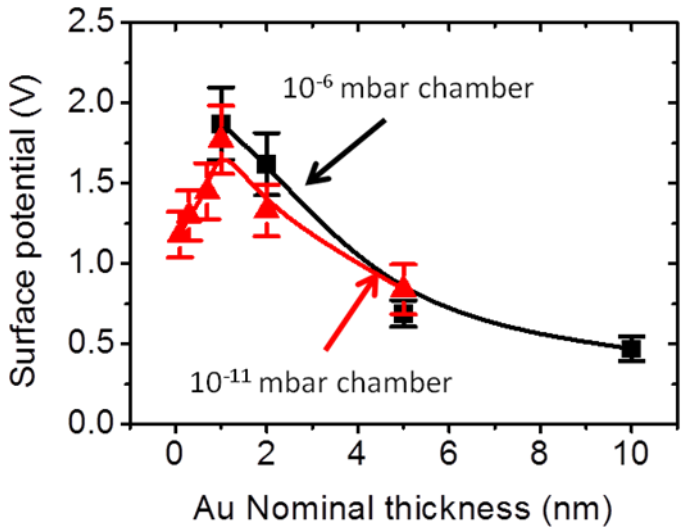

Fig. 4: Surface potentials after venting with air

3.3 Morphology of Au on graphite

A look at the TEM micrographs of the Au films on graphite may be seen in Figure 5. At first, films are made up of individual nanoparticles and are therefore discontinuous. Approximating spherical geometry and measuring across their diameter allowed us to establish the particle sizes. With increasing particle density, the average distance between closest neighbors shrank exponentially. Distributions shown by histograms (inset) reveal

coalescence was the dominant process, with the islands finally merging into a single film.

ISSN: 2348-1358
Impact Factor: 6.901
NAAS Rating: 3.77

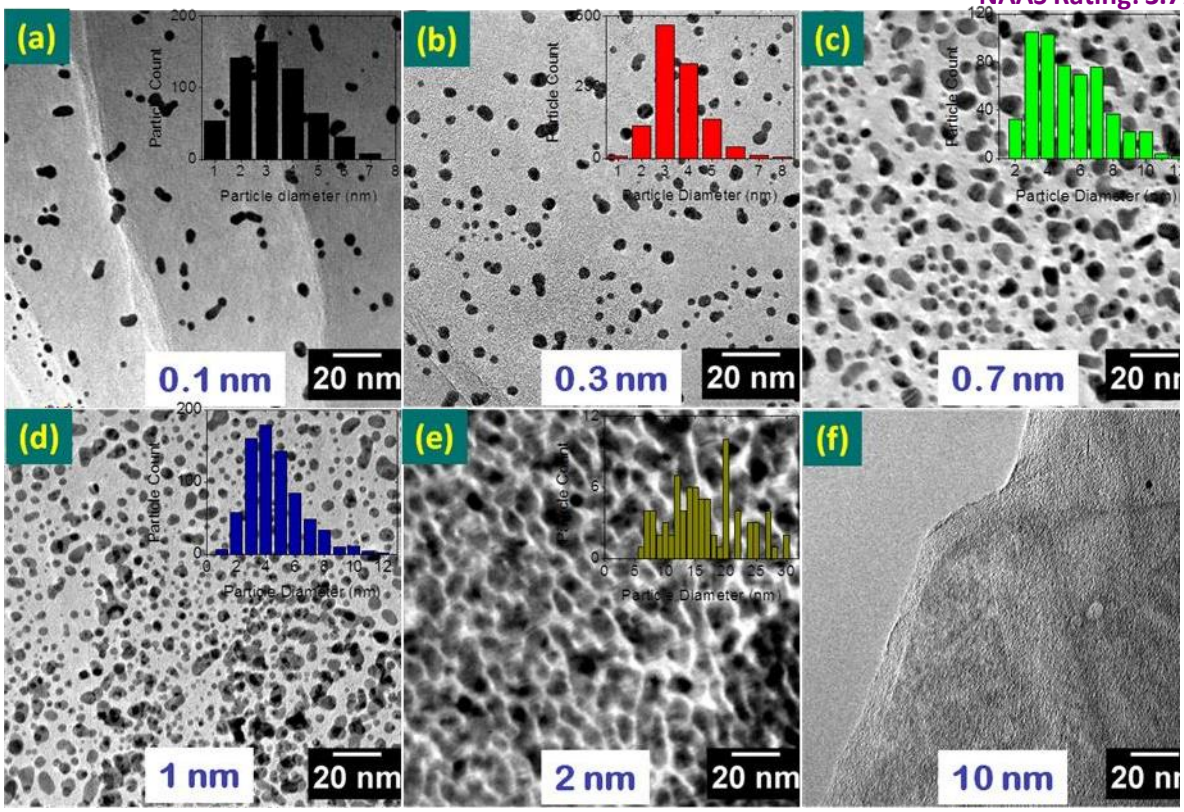

Fig. 5: TEM micrographs of gold on graphite (a) 0.1 nm (b) 0.3 nm (c) 0.7 nm (d) 1 nm (e) 2 nm and (f) 10 nm. (Inset: Histogram distribution of approximated particle widths)

3.4 Effects of contacting Pt and Cr on surface potential

As seen in Figure 6a, 1 nm Pt on graphite nanostructures exhibit an SP value of 2 V and then undergo exponential decline. When the film thickness was greater than 10 nm, the potentials recorded with Pt tips converged to 0.06 V and those with Au tips to 0.5 V. Identical to Au deposition, this pattern emerged. A sign inversion of -2 V was found on a 1 nm thick sample when Cr was deposed (Fig. 6b). The SP converged to -0.9 V and -0.65 V, respectively, were measured with Pt and Au tips, for thicknesses greater than 10 nm. The transmission electron microscopy (TEM) examinations shown in Figure 6 (c and d) also showed comparable nanoparticle morphologies. When compared to Au with a comparable deposition, the particles were denser and smaller. The films were certified to be polycrystalline by SAED (inset) for both of them. We see significant relationships with Au, despite the fact that sub-nanometer Pt and Cr films could not be deposited. I. The potential rises with metal nanoparticles and the AFM tip employed; (ii) the value decreases exponentially with metal coverage;

ISSN: 2348-1358
Impact Factor: 6.901
NAAS Rating: 3.77

and (iii) the constant value on thick films relies on the metal. After releasing air from the apparatus, the patterns remained same.

ISSN: 2348-1358
Impact Factor: 6.901
NAAS Rating: 3.77

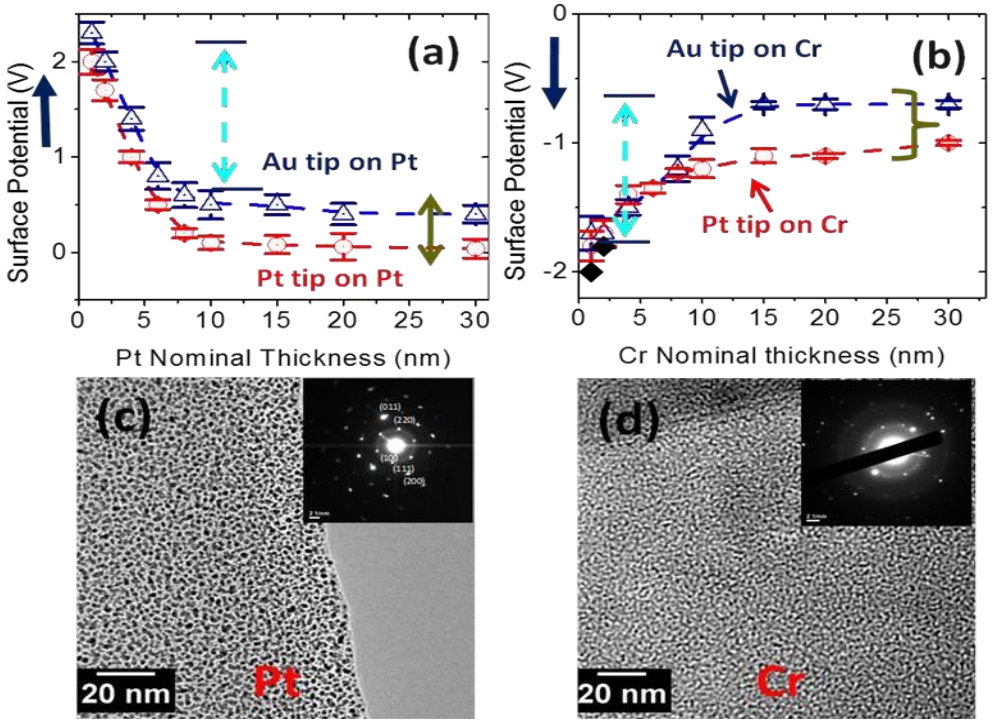

Fig. 6. Surface potential on (a) Pt and (b) Cr, (c) and (d) Corresponding TEM micrographs for 1 nm deposition (inset: SAED pattern).

4.0 Discussion

4.1 Growth of metal films on graphite

Thin film evolution is supported by the change in film shape (Fig. 5; NETTERFIELD and Martin, 1986; Tang, 2003). When atoms touch the surface of graphite, they move quickly enough to nucleate with other atoms, creating nanoparticles. Clusters move more easily and agglomerate more effectively when electrostatics are used. Several nucleation spots are produced during deposition, leading to an increase in particle density. Eventually, the islands come together to form a continuous film. Figure

The measured width is widened by the considerable curvature of the AFM tip, which causes the apparent particle heights from topography scans (Fig. 1) to be much bigger than the true cluster sizes (Fig. 5).

ISSN: 2348-1358
Impact Factor: 6.901
NAAS Rating: 3.77

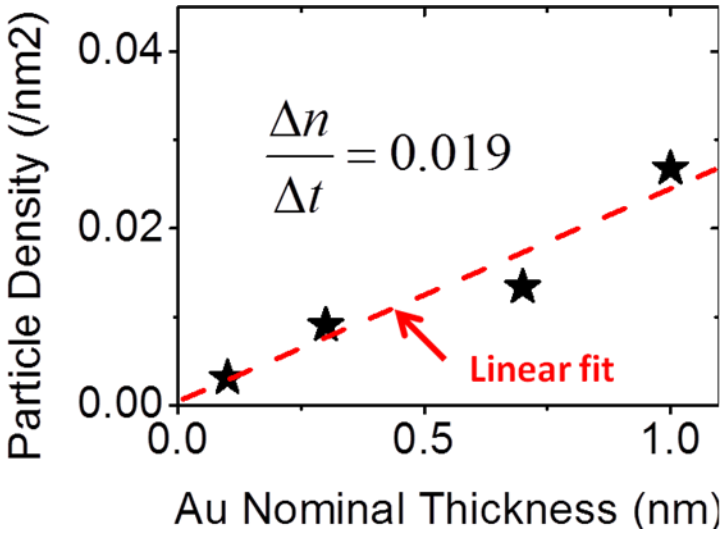

Fig. 7. Variation of particle density with Au nominal thickness

4.2 Electronic structure of metal-graphite interfaces

The corresponding theoretical work function differences on fresh graphite with Pt tips are 0.95 V and 0.45 V, respectively, whereas the observed values on Au tips are 0.45 V. According to Michaelson (1950), Sze (1981), and Michaelson (1978), the first modifications on metal deposits are obviously greater than the related work function. The assumption that topographical heights are mostly impacted by tip convolution is supported by the absence of obvious association in Fig. 1 between apparent particle heights from topography and potentials. Charge distribution on the sample is represented by SP measurements, which, on the other hand, are average local values (Zerweck et al., 2005; Pandey et al., 2008; Lu et al., 2006). This has no effect on the spatial resolution and only changes the lateral resolution of individual particles. This is supported by the fact that SP values on thin films are metal dependent, yet they remain constant when measured with various metal tips, suggesting that the sample electronic states have changed. Dipole interactions on certain particles cause huge peak-to-peak changes; these interactions just raise the margin of error; overall trends are preserved.

The effects of the work function difference (VWFD), charge transfer (Vtransfer), and bonding interaction (Vbonding) between the surface of the metal and graphite may be modeled in potential measurements.

"Transfer" is the result of multiplying V with WFD.

one (1)

ISSN: 2348-1358
Impact Factor: 6.901
NAAS Rating: 3.77

For the same metal, both □VWFD and □Vbonding remain constant. This means that the modifications would result from sample charging, which is defined as follows (Giovannetti et al., 2008):

Vmeasured denotes

□ e.N □

two (2)

0

where is the permittivity of empty space, N is the number of electrons transported per unit area, and e is the charge of each electron. Dipoles allow us to picture the charges emanating from individual particles, which may be expressed as:

$$\square V_{measured} \quad \square \quad \frac{1}{4\square\square} \quad \square\Sigma P.n\square \qquad (3)$$

0

A particle's dipole moment (P) and the direction normal to the field (n) are defined here. Fig. 8, which displays the surface potentials with nominal thickness, demonstrates that the variations in SP are clearly correlated with the average particle density, as shown by:

$$\square V_{measured} \quad \square \quad 29.47\square n \qquad (4)$$

Where □*n* is the particle density.

ISSN: 2348-1358
Impact Factor: 6.901
NAAS Rating: 3.77

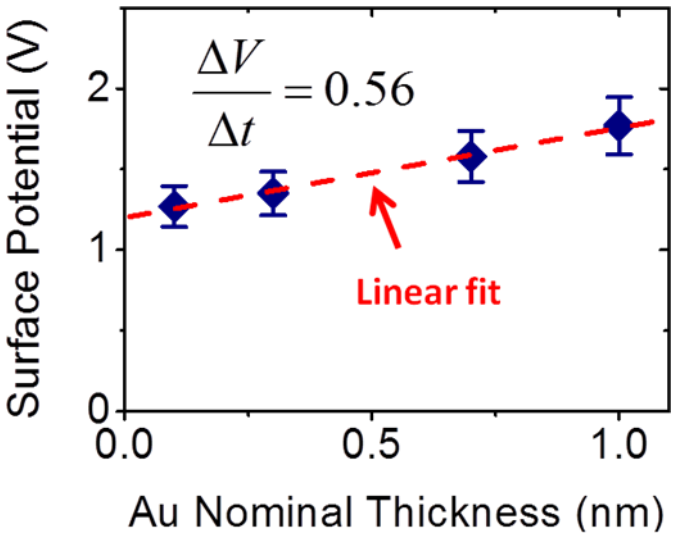

Fig. 8. Variation of surface potential with gold nominal thickness

As seen in Figure 9, the metal tip is affected by the dipole field underneath it because graphite conducts solely along the c-axis. Nevertheless, the area occupied by a single nanoparticle is far less than the cantilever.

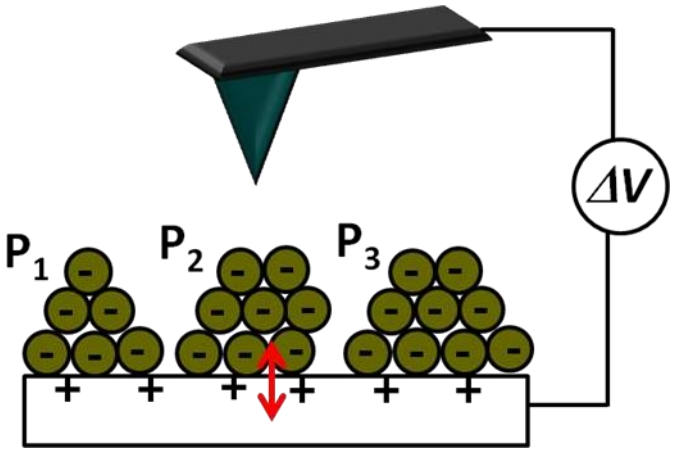

Fig. 9. Schematic illustration of charge symmetry of metal nanoparticles on graphite

$$\Delta V \quad \Delta \frac{e.P}{A} \quad \text{——} \quad (5)$$

transfer

The relation shown in Table 1 may be used to estimate the charge at the Au-graphite contact. This means that more atoms on the surface are accessible to interact with the graphite surface as the particle

ISSN: 2348-1358
Impact Factor: 6.901
NAAS Rating: 3.77

density increases. As a result, the transmission of charges is enhanced. On the other hand, the 1.1 eV calculated for uniform monolayer coverage of Au on graphite by Giovannetti et al. (2008) is much larger than these estimates. We think that the closest arrangement of Au atoms is responsible for this variation. According to the work function of the metal, the direction of charge transfer is dictated by the initial change in sign (Giovannetti et al., 2008; Liu et al., 2011; Jin et al., 2010). Electrons travel from graphite to metals like Au and Pt because their work functions are greater than graphite's. Because of this, the surface of the graphite is negatively doped with Cr, as Cr has a lower work function than graphite.

Table 1: Calculated charging associated with average dipole per nanoparticle

Au Thickness (nm)	$\square V_{measured}$ *(V)*	*Dipole moment (D)*	$\square V_{transfer}$ *(eV)*
0.1	0.3	0.34	0.04
0.3	0.38	0.54	0.06
0.7	0.61	1.4	0.16
1	0.80	2.41	0.27

ISSN: 2348-1358
Impact Factor: 6.901
NAAS Rating: 3.77

Because the charged interface is buried below the surface, dipole effects are decreased, causing potentials to converge to a constant value for thick films. As a result, the conduction band is the space where electrons in the bulk metal layer may flow. Thus, the observed values are a consequence of the interaction between the metal film's electrons and the AFM tip's electrons. This follows from the fact that the work function of the metal tip is different from that of the metal in its bulk.

5.0 Conclusion

It has been discovered that the surface potential of graphitic nanostructures that are in contact with ultrathin films of gold, platinum, or chromium varies with the nanoparticle size and the kind of metal. The values for gold and platinum reached 1.4 V, which is much more than the bulk metal values of 0.45 V and 0.6 V, respectively. With a value of -2 V for tiny nanoparticles and -0.9 V for bulk chromium, a sign inversion is seen for chromium. It has been shown that an inversion in the graphite Fermi level, in agreement with known doping characteristics, is responsible for the change in sign of the work function. The charge transfer from the metal nanoparticles to the graphitic nanostructure has been confirmed by calculating the resultant surface dipole. With nanoparticles placed between 0.1 nm and 1 nm in nominal thickness, the charge transfer rose from 0.04 eV to 0.27 eV. These findings demonstrate that morphology, in addition to metal choice, may be used to adjust the electrical structure on graphite surfaces. Catalysis on support and graphene/graphite devices are greatly affected by this.

References

This sentence was paraphrased from an article by Benayad et al. (2009). Improving the reduced graphite oxide's work function by manipulating the concentration of Au ions. Journal of Chemical Physics, 475 (1-3), 91-95.
Martin I and Blanter Y (2007). Movement using typical metalgraphene interfaces.
Article number: 155433 in Physical Review B, volume 76, issue 15.

Ohta T, Brar V, Bostwick A, Crommie (2007), yayon Y, Zhang Y, McChesney J, Rotenberg E, and Horn K. Examining the non-uniform electrical structure of monolayer and bilayer graphene on SiC using scanning tunneling spectroscopy. Publication: Applied Physics Letters, Volume 91, Issue 12, Pages 122–122.
Laibowitz R, Viggiano (1986), Gefen Y, and Shih W. The region around the percolation metal-insulator transition exhibits nonlinear behavior. Physical review letters, volume 57, issue 24, pages 3097–3100.
As published in 2008 by Giovannetti G, Khomyakov P, Brocks G, Karpan V, van den Brink J, and Kelly P. Incorporating metal contacts into graphene. Review of Physical Research, 101(2), 26803.
The work of Gomer R. from 1975. Interactions on surfaces of metals? Berlin, Germany: Springer-Verlag

Heidelberg.
In 2010, Gong, Lee, Shan, Vogel, Wallace, and Cho published their work. An investigation on the interfaces between metalgraphene based on first principles. No. 108, page 123711, Journal of Applied

ISSN: 2348-1358
Impact Factor: 6.901
NAAS Rating: 3.77

Physics.
Hunderi O. and Granqvist C. (1978). Ultrafine metal particle selective solar energy absorption: model-based calculations. The citation is from the Journal of Applied Physics(50), 1058.
Otani M. and Hamada I. (2010). A van der Waals density-functional analysis of graphene on metallic surfaces that is comparative. Journal of Physical Review B, 82(15), 153412.

The authors of the 2008 study are Huard, Stander, Sulpizio, and Goldhaber-Gordon. Proof that contacts are responsible for the electron-hole imbalance in graphene. Publication: Physical Review B, Volume 78, Issue 12, Page 121142.
In 2010, Jin, Choi, and Jhi published a work. Alkali metal adsorption on graphene: a crossover phenomenon. The reference for this article is Physical Review B, volume 82, issue 3, reference 033414.
Leonardo da Vinci and Kelvin G. (1898). Issue 46 (80) of Philosophy Magazine.
As stated in the 2009 publication by Klusek, Dabrowski, Kowalckyk, Kozlowski, Olejniczak, Blake, and Szybowicz. Scanning tunneling spectroscopy in the study of electron densities in graphene on gold. Article cited as 95 (11), 113114-113114 in Applied Physics Letters.

Authors: Li G., Luican A., and Andrei E. Scanning Tunneling Spectroscopy of Graphene on Graphite. Article number: 176804 in the Physical Review Letters.
Huang, Liu, and Zhu (2011). Adding chemical doping to graphene. Article number: 3335 in the Journal of Materials Chemistry, volume 21, issue 10.
The authors of the 2006 study were Lu Y, Munoz M, Steplecaru C, Hao C, Bai M, Garcia N, Schindler K, and Esquinazi P. Coexistence of Insulating and Conducting Behaviors on Oriented Graphite Surfaces: Electrostatic Force Microscopy. "Physical Review Letters" (97, no. 7, pages 1-4).

It was published in 2007 by Marchini, Gunther, and Wintterlin. Electron scanning tunneling microscopy of graphene on Ru (0001). Review of Physical Research B, 76(7), 075429.
In 1950, Michaelson H. Work Functions of the Elements. Paper number 536 in the journal Inorganic Chemistry. Johannsson H. (1978). Atomic functions and periodicity in their work.
Article number: 4729 in the Journal of Applied Physics, volume 48, issue 11.
Robert Netterfield and Paul Martin in 1986. Gold films made by evaporation and ion-assisted deposition: nucleation and growth investigations. Surface science with an applied focus, 25, 265-278.
In 2002, Obraztsov, Volkov, Boronin, and Kosheev published a work. Publication: Diamond and associated materials, 11, 813-818.
Published in 2003 by Ohgi and Fujita. Single electron charging electron effects in gold nanoclusters on alkanedithiol layers with varying molecular lengths.
Article published in Surface Science, 532, pages 294-299.
In 2008, Pandey, Reifenberger, and Piner published a paper. Investigating exfoliated oxidized graphene sheets using scanning probe microscopy methods. Article published in Surface Science, volume 602 issue 9, pages 1607–1613.
This was written by Pirkle, Wallace, and Colombo in 2009. Investigations of graphite dielectrics using Al2O3 and HfO2 in situ. Journal of Applied Physics, 95, 133106.

ISSN: 2348-1358
Impact Factor: 6.901
NAAS Rating: 3.77

The authors of the 2010 study were Rusu, Giovannetti, Weijtens, Coehoorn, and Brocks. Investigation of the development of dipole layers at metal-organic interfaces using first-principles calculations. Review of Physical Research B, 81 (12), 125403.
The year 1981 was stated by Somorjai G. Surface chemistry and catalysis: an overview. North America: Wiley.
Song X, Lu J, and Sun Z (2010). Using ultrahigh vacuum nc-AFM to observe silicon surfaces. No. 85, issue 2, pages 297–301, vacuum.
E. Sutter, P. Sutter, and J. Flege (2008). Ruthenium coated with epitaxial graphene. Seventh edition, issue 5, pages 406-411, appearing in Nature Materials.

(1981) by SSze. Physics of Semiconductor Devices. North America: Wiley.
According to Tang (2003). Gold substrate surface roughness and resistivity. Publication: Microelectronic Engineering, Volume 66, Issues 1-4, Pages 445–450.
Lu (2008), Uchoa B, and Neto A. Adding metal coatings to graphene by hand. Publication: Physical Review B, Volume 77, Issue 3, CITATION: 035420.

This work was published in 2005 by Zerweck, Loppacher, Otto, Grafstrom, and Eng. Kelvin probe force microscopy: precision and resolution limitations. Paper published in Physical Review B, volume 71, issue 12, pages 1–9.